

# Analytical Forced Convection Modeling of Plate Fin Heat Sinks

P. Teertstra, M.M. Yovanovich and J.R. Culham

Microelectronics Heat Transfer Laboratory  
Department of Mechanical Engineering  
University of Waterloo  
Waterloo, Ontario, Canada

and

T. Lemezyk

R-Theta Inc.  
Mississauga, Ontario, Canada

## ABSTRACT

An analytical model is presented that predicts the average heat transfer rate for forced convection, air cooled, plate fin heat sinks for use in the design and selection of heat sinks for electronics applications. Using a composite solution based on the limiting cases of fully-developed and developing flow between isothermal parallel plates, the average Nusselt number can be calculated as a function of the heat sink geometry and fluid velocity. The resulting model is applicable for the full range of Reynolds number,  $0.1 < Re_b^* < 100$ , and accurately predicts the experimental results to within an RMS difference of 2.1%.

## NOMENCLATURE

|           |   |   |
|-----------|---|---|
| $A$       | = | channel surface area, $\equiv 2LH$ , $m^2$  |
| $A_a$     | = | approach flow cross section area, $m^2$     |
| $A_c$     | = | fin cross section area, $\equiv tL$ , $m^2$ |
| $A_o$     | = | heat sink flow cross section area, $m^2$    |
| $b$       | = | channel spacing, $m$                        |
| $c_p$     | = | specific heat, $J/kgK$                      |
| $C_1$     | = | radiation correlation coefficient, $W/K^4$  |
| $Gz$      | = | Graetz number                               |
| $h$       | = | average heat transfer coefficient, $W/m^2K$ |
| $H$       | = | fin height, $m$                             |
| $k$       | = | fin thermal conductivity, $W/mK$            |
| $k_f$     | = | fluid thermal conductivity, $W/mK$          |
| $L$       | = | fin, baseplate length, $m$                  |
| $\dot{m}$ | = | mass flow rate, $kg/s$                      |
| $m$       | = | fin parameter, $1/m$                        |
| $n$       | = | composite model combination parameter       |
| $N$       | = | number of fins                              |

|          |   |  |
|----------|---|--|
| $Nu_b$   | = | Nusselt number, $\equiv (Qb)/(k_f A(T_s - T_a))$       |
| $Nu_i$   | = | ideal Nusselt number, $\eta = 1$                       |
| $P$      | = | fin perimeter, $\equiv 2t + 2L$ , $m$                  |
| $Pr$     | = | Prandtl number, $\equiv \nu/\alpha$                    |
| $Q$      | = | total heat transfer rate, $W$                          |
| $Re_b$   | = | Reynolds number, $\equiv Ub/\nu$                       |
| $Re_b^*$ | = | channel Reynolds number, $\equiv Re_b \cdot (b/L)$     |
| $T_a$    | = | inlet air temperature, $^{\circ}C$                     |
| $T_f$    | = | film temperature, $\equiv (T_s + T_a)/2$ , $^{\circ}C$ |
| $T_s$    | = | baseplate temperature, $^{\circ}C$                     |
| $T_w$    | = | fin temperature, $^{\circ}C$                           |
| $t$      | = | fin thickness, $m$                                     |
| $U$      | = | average velocity in channel, $m/s$                     |
| $W$      | = | baseplate width, $m$                                   |

## Greek Symbols

|          |   |                              |
|----------|---|------------------------------|
| $\alpha$ | = | thermal diffusivity, $m^2/s$ |
| $\eta$   | = | fin efficiency               |
| $\nu$    | = | kinematic viscosity, $m^2/s$ |
| $\rho$   | = | mass density, $kg/m^3$       |

## Subscripts

|       |   |                                |
|-------|---|--------------------------------|
| $fd$  | = | fully-developed flow asymptote |
| $dev$ | = | developing flow asymptote      |
| $tot$ | = | total                          |
| $r$   | = | radiation component            |

## INTRODUCTION

Finned heat sinks are commonly used devices for enhancing heat transfer from air cooled microelectronics and power electronics components and assemblies. The use of finned heat sinks increases the effective

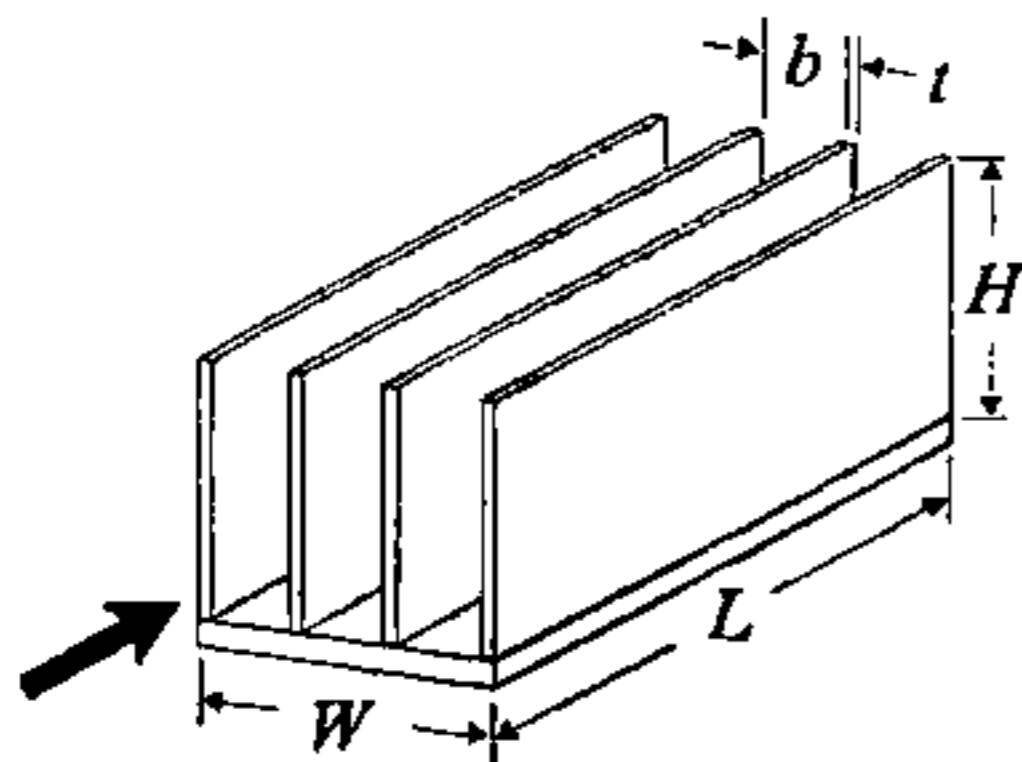


Fig. 1 Schematic of Plate Fin Heat Sink Geometry

surface area for convective heat transfer, reducing the thermal resistance and operating temperatures in air-cooled electronics. The plate fin heat sink shown in Fig. 1 is one of the most common configurations used in current applications. It consists of a parallel, uniform array of thin, conductive plates of length  $L$ , height  $H$  and thickness  $t$ , mounted on a baseplate of dimensions  $L \times W$ . Heat is convected from the heat sink by fan or blower-driven airflow through the channels formed between the fins in a direction parallel to the baseplate.

The task of selecting the best heat sink for a particular application from the hundreds of configurations available from the various manufacturers can be a formidable task for an engineer. The choice of an optimal heat sink depends on a number of factors, including the performance, dimensional constraints, the available airflow, and cost, where the optimum configuration provides the best balance between all of these factors. In order to optimize these parameters, design tools are required that quickly and easily predict heat sink performance early in the design process, prior to any costly prototyping or time-consuming detailed numerical studies.

A number of studies of forced convection for an array of parallel plates with applications for the plate fin heat sink are currently available in the literature. Sparrow, Baliga and Patankar [1] present an analytical study for a forced convection cooled, shrouded plate fin array, and present their results for the average heat transfer rate in tabular form. Wirtz, Chen and Zhou [2] present a study of flow bypass effects on plate fin heat sinks, and recommend the use of the developing flow correlation of Shah and London [3], which is modified from its original, log-mean temperature formulation. Lee [4] also recommends the use of a developing flow correlation with his fit of parallel-plate data presented in Kays and London [5], but no general model or correlation is provided. Kraus and

Bar-Cohen [6] recommend the use of fully-developed laminar and turbulent pipe flow correlations for predicting the average heat transfer coefficient but do not present any models for developing flow. There are currently no simple models available in the literature that are applicable to both fully-developed and developing flows.

The objective of this study is to present an analytical, forced convection model for the average heat transfer rate from a plate fin heat sink for the full range of Reynolds number, from fully-developed to developing flow. The proposed model includes fin effects to compensate for a temperature variation between the fins and the baseplate, which can have a substantial influence on the performance of high aspect ratio heat sinks. Experimental measurements are performed for an air-cooled heat sink prototype, and these results will be used to validate the proposed model.

## MODEL DEVELOPMENT

### Problem Definition

The problem of interest in this study involves forced convection heat transfer for a plate fin heat sink, a parallel uniform array of  $N$  plates of thermal conductivity  $k$  mounted to a conductive baseplate, with dimensions as shown in Fig. 1. The baseplate is assumed to be relatively thick and composed of a high conductivity material, such that spreading resistance effects can be neglected and the baseplate can be treated as isothermal. The lower surface and edges of the baseplate will be assumed adiabatic, which should provide a conservative estimate of the performance of the heat sink.

This analysis will assume a uniform velocity of magnitude  $U$  through the channels formed between the fins, with no "leakage" of air out the edges of the channels. This condition is achieved physically by placing a shroud on top of the fins, such that all airflow is contained within the channels. This assumption of uniform velocity may also be used in conjunction with models for flow bypass for unshrouded heat sinks, such as those presented by Wirtz, Chen and Zhou [2] or Simons and Schmidt [7].

The heat sink will be modeled as  $N - 1$  parallel plate channels, with each channel defined as shown in Fig. 2 with uniform inlet velocity  $U$  and ambient fluid temperature  $T_a$  specified at the channel inlet. To simplify the analysis, the ends of the channel formed by the shroud and baseplate are treated as adiabatic, zero

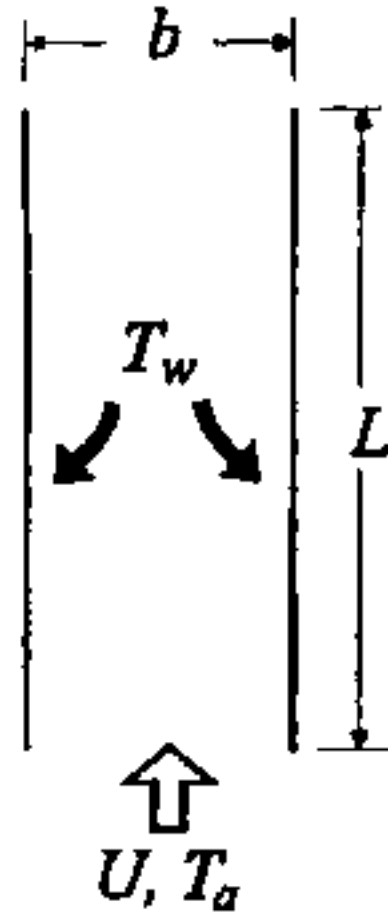


Fig. 2 Schematic of Two-Dimensional Channel

shear surfaces, such that the flow field becomes two-dimensional. This assumption is valid for  $b \ll H$ , such as in high aspect ratio manufactured heat sinks used for power electronics of other high heat flux applications. The accuracy of this modeling approach may be questionable for larger fin spacing,  $b \approx H$ , where the effects of the baseplate and the shroud cannot be neglected.

In the first step of the modeling procedure a uniform temperature boundary condition,  $T_w = T_s$ , is imposed on each of the channel walls to determine the functional relationship for the average heat transfer coefficient for the simple, 2D channel problem. The second part of the modeling procedure uses a fin analysis to predict the actual heat transfer rate from the heat sink based on the behavior of the ideal channel and as a function of the fin dimensions and thermal conductivity.

All air properties will be calculated at the film temperature:

$$T_f = \frac{T_s + T_a}{2}$$

Both the independent and dependent variables are non-dimensionalized using the channel width  $b$  as the characteristic length. The Reynolds number is defined as:

$$Re_b = \frac{U b}{\nu} \quad (1)$$

The dimensionless average heat transfer rate is expressed in terms of the Nusselt number defined as:

$$Nu_b = \frac{Q b}{k_f A (T_s - T_a)} \quad (2)$$

where  $Q$  is the total heat transfer from both channel walls and  $A$  is the total area  $A = 2 L H$ .

### Parallel Plate Channel

The problem of forced convection heat transfer between isothermal parallel plates is well documented in the literature for the two limiting cases, fully-developed flow and simultaneously developing thermal and hydrodynamic flow. These two limiting cases will be used as asymptotic solutions for small and large  $Re_b$  in a general model for all values of the independent parameter. These asymptotes are combined using the inverse form of the Churchill and Usagi [8] composite solution technique:

$$Nu_b = \left[ \left( \frac{1}{Nu_{fd}} \right)^n + \left( \frac{1}{Nu_{dev}} \right)^n \right]^{-1/n} \quad (3)$$

where  $Nu_{fd}$  and  $Nu_{dev}$  are the asymptotic solutions for fully-developed and developing flow, respectively. The combination parameter  $n$  is used to control the behavior of the model in the transition region between the asymptotes, and its value will be determined based on empirical results.

Due to the relatively large heat transfer coefficients achieved in forced convection flows, it is anticipated that fin effects will be an important factor in predicting average heat transfer from the heat sink. The proposed model will include fin effects, but will address them later in the analysis. At this point in the development of the model the channel walls are assumed to be isothermal and of equal temperature to the baseplate,  $T_w = T_s$ .

### Fully-Developed Flow Asymptote

In their study of optimal spacing for forced convection cooled parallel plates, Bejan and Sciubba [9] suggest that the asymptotic value of  $Nu_b$  for fully-developed flow occurs when the average temperature of the air exiting the channel equals the wall temperature  $T_s$ . For this condition, it can be shown through an enthalpy balance on the fluid passing through the channel that:

$$Q = \dot{m} c_p (T_s - T_a) \quad (4)$$

The mass flow rate can be expressed in terms of the channel cross sectional area and the average velocity:

$$Q = \rho c_p (b H) U (T_s - T_a) \quad (5)$$

Non-dimensionalizing with the previously defined Nusselt and Reynolds numbers gives:

$$Nu_b = \frac{1}{2} \frac{b}{L} Re_b Pr \quad (6)$$

The channel width, length and Reynolds numbers are combined to form a single, dimensionless value analogous to the channel, or Elenbaas Rayleigh number for natural convection. The channel Reynolds number is defined as:

$$Re_b^* = Re_b \cdot \frac{b}{L} \quad (7)$$

Using this relation, the fully-developed asymptote becomes:

$$Nu_{fd} = \frac{1}{2} Re_b^* Pr \quad (8)$$

### Developing Flow Asymptote

A number of analytical models and correlations are currently available in the heat exchanger literature for simultaneously developing flow in isothermal ducts; however most of these studies are based on a log-mean or local temperature difference between the fluid and the boundary. Sparrow [10] presents an integral solution for laminar forced convection in the entrance region of flat, rectangular ducts, and includes a formulation for the average Nusselt number based on the inlet temperature:

$$Nu_{D_e} = \frac{0.664 Gz_{D_e}^{1/2}}{Pr^{1/6}} \left[ 1 + 7.3 \left( \frac{Pr}{Gz_{D_e}} \right)^{1/2} \right]^{1/2} \quad (9)$$

valid for  $Pr \approx 1$ . For a channel length  $L$ , the Graetz number is defined as:

$$Gz_{D_e} = \frac{Re_{D_e} Pr}{L/D_e} \quad (10)$$

where the effective diameter  $D_e$  for parallel plates is equivalent to  $2b$ . The developing flow expression is converted in terms of the previously defined dimensionless parameters to give the developing flow asymptote:

$$Nu_{dev} = 0.664 \sqrt{Re_b^*} Pr^{1/3} \left( 1 + \frac{3.65}{\sqrt{Re_b^*}} \right)^{1/2} \quad (11)$$

At the limit of large  $Re_b^*$  this asymptote can be shown to approach the classical isothermal flat plate solution:

$$Nu_L = 0.664 \sqrt{Re_L} Pr^{1/3}$$

### Composite Model

The asymptotes developed in the previous sections for fully-developed and developing channel flow are combined using the composite model, Eq. (3), to give:

$$Nu_b = \left[ \frac{1}{\left( \frac{Re_b^* Pr}{2} \right)^n} + \frac{1}{\left( 0.664 \sqrt{Re_b^*} Pr^{1/3} \sqrt{1 + \frac{3.65}{\sqrt{Re_b^*}}} \right)^n} \right]^{-1/n} \quad (12)$$

The plot in Fig. 3 shows the behavior of these two asymptotes, along with the composite model for the full range of  $Re_b^*$  from developing to fully-developed flow. The proposed composite model approaches the limiting cases for small and large values of  $Re_b^*$  and predicts a smooth transition in the intermediate region:

$$3 < Re_b^* < 20$$

The optimized value of the combination parameter,  $n$ , in Eq. (12) is determined using data from a numerical solution of the two-dimensional channel problem. Numerical simulations were performed using FLOTHERM [11], a commercial, finite volume-based CFD package. A simple two-dimensional channel was modeled using an isothermal, no-slip boundary to simulate the walls and a uniform velocity distribution at the inlet. Five cases were examined which span the full range of the independent parameter:

$$0.26 \leq Re_b^* \leq 175$$

The results of these numerical simulations are shown along with the proposed model in Fig. 4. Based on this comparison of the model with the numerical data,

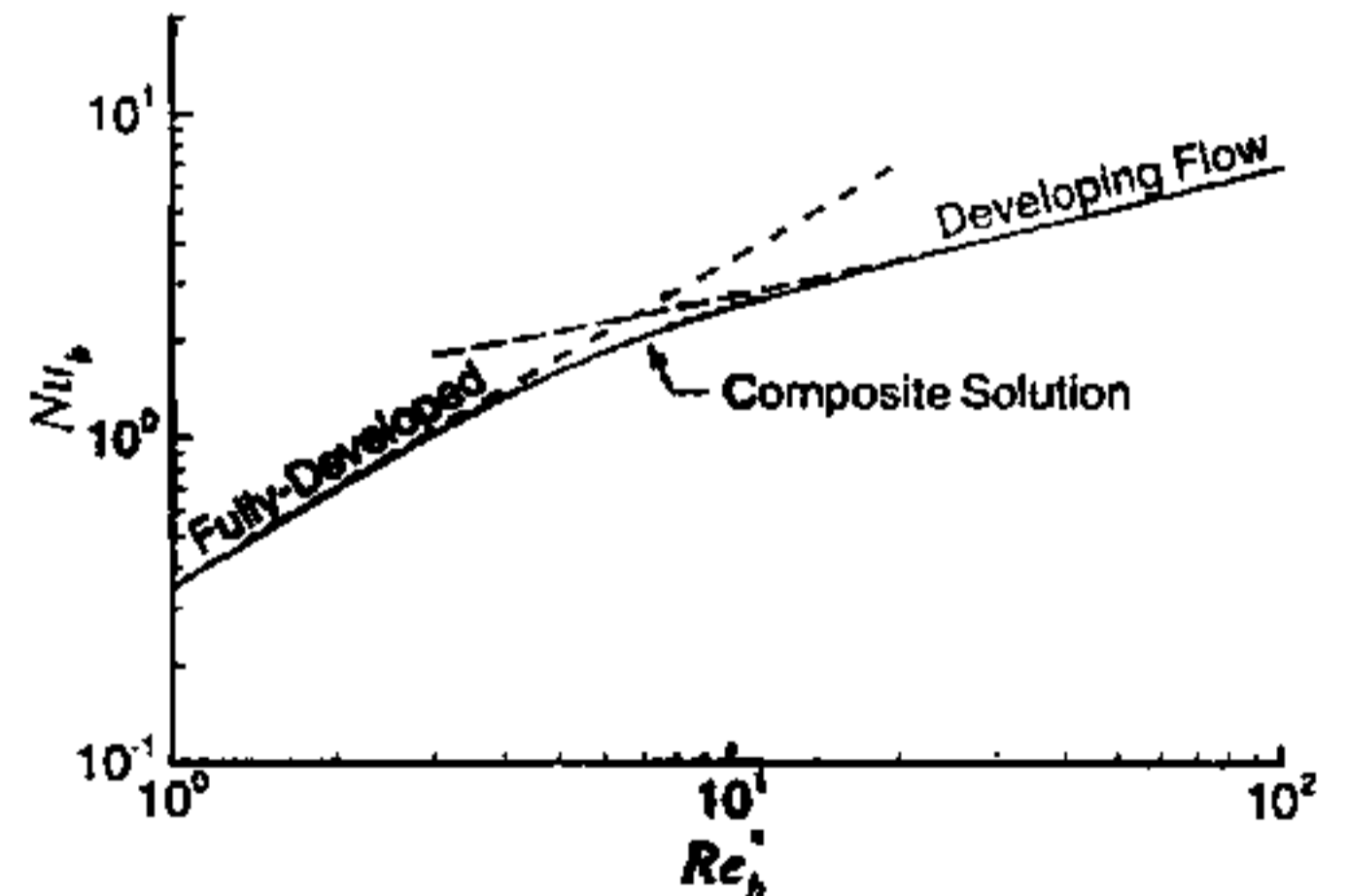


Fig. 3 Proposed Solution Behaviour



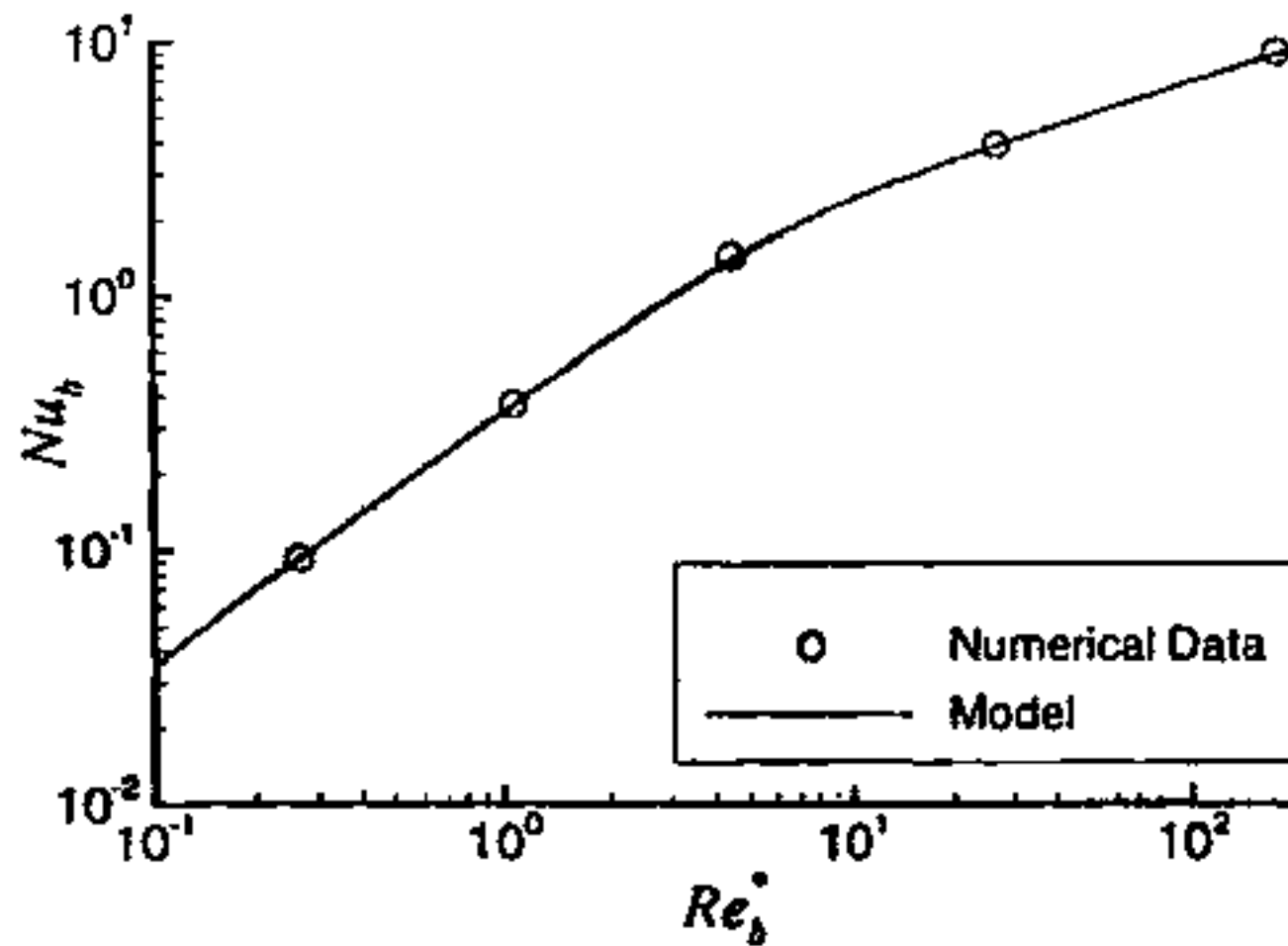


Fig. 4 Comparison of Model and Numerical Results for 2D Channel

a value for the combination coefficient of  $n = 3$  was determined which minimizes the difference between the model and numerical predictions over the full transition region. When  $n = 3$ , the RMS percent difference between the model and the numerical data is 2.1%.

### Fin Effects

The goal in high aspect ratio heat sink configurations is to maximize the available fin surface area, which is often achieved at the expense of fin efficiency. As the fins become taller and thinner, the temperature difference between the fins and the baseplate increases due to the increased conductive resistance, and the performance of the heat sink is reduced. This effect is more pronounced for forced convection, where strong convection on the fins tends to remove heat more quickly than it can be replaced through conduction from the baseplate. The proposed model for the plate fin heat sink must take these effects into account.

The analytical model for the parallel plate channel developed in the previous section assumes that the fin temperature is equal to that of the baseplate,  $T_w = T_b$ , resulting in the largest possible heat transfer values. Treating the model predictions as ideal values,  $Nu_i$ , the fin efficiency  $\eta$  is defined by:

$$\eta = \frac{Nu_b}{Nu_i} \quad (13)$$

where  $Nu_b$  is the average heat transfer rate for  $T_w < T_b$ . Assuming an adiabatic condition at the fin tip, the efficiency can be determined as follows [12]:

$$\eta = \frac{\tanh(mH)}{mH} \quad (14)$$

where  $H$  is the height of the fin and  $m$  is defined as:

$$m = \sqrt{\frac{hP}{kA_c}} \quad (15)$$

The perimeter  $P$  and cross sectional area  $A_c$  of the fins are given by:

$$P = 2t + 2L, \quad A_c = tL$$

and  $k$  is the thermal conductivity of the fin material. The average heat transfer coefficient  $h$  can be related to the ideal value of Nusselt number by:

$$h = Nu_i \cdot \frac{k_f}{b} \quad (16)$$

Substituting these expressions into Eq. (14) and simplifying yields:

$$\eta = \frac{\tanh \sqrt{2Nu_i \frac{k_f}{k} \frac{H}{b} \frac{H}{t} \left( \frac{t}{L} + 1 \right)}}{\sqrt{2Nu_i \frac{k_f}{k} \frac{H}{b} \frac{H}{t} \left( \frac{t}{L} + 1 \right)}} \quad (17)$$

The "ideal" fin, with  $\eta = 1$  is approached when the argument of the  $\tanh(\cdot)$  function and the denominator both approach zero:

$$\lim_{x \rightarrow 0} \frac{\tanh(x)}{x} = 1$$

It can be shown that changes to the value of the parameters in Eq. (17) that would decrease the conductive resistance in the fin, such as a decrease in  $H/b$ ,  $H/t$ , or an increase in  $k$ , would tend to reduce the value of the argument, resulting in fin efficiency approaching the ideal fin,  $\eta = 1$ .

### Model Summary

Combining the fin efficiency from Eq. (17) with the solution for the parallel plate channel, the composite model for forced convection for the plate fin heat sink is:

$$Nu_b = \frac{\tanh \sqrt{2Nu_i \frac{k_f}{k} \frac{H}{b} \frac{H}{t} \left( \frac{t}{L} + 1 \right)}}{\sqrt{2Nu_i \frac{k_f}{k} \frac{H}{b} \frac{H}{t} \left( \frac{t}{L} + 1 \right)}} \cdot Nu_i \quad (18)$$

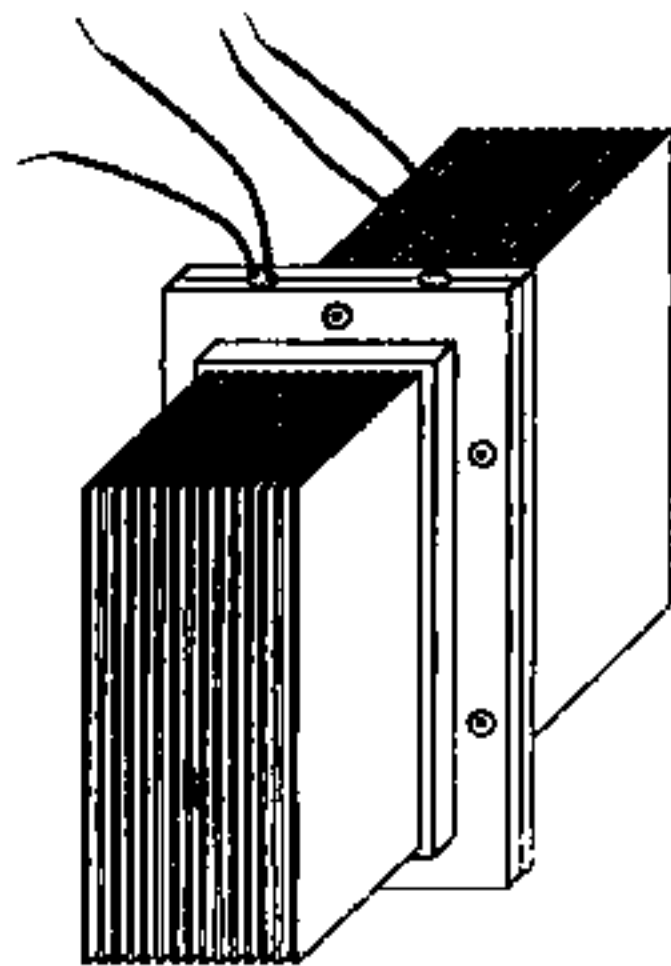


Fig. 5 Back-to-back Heat Sink Prototype Assembly

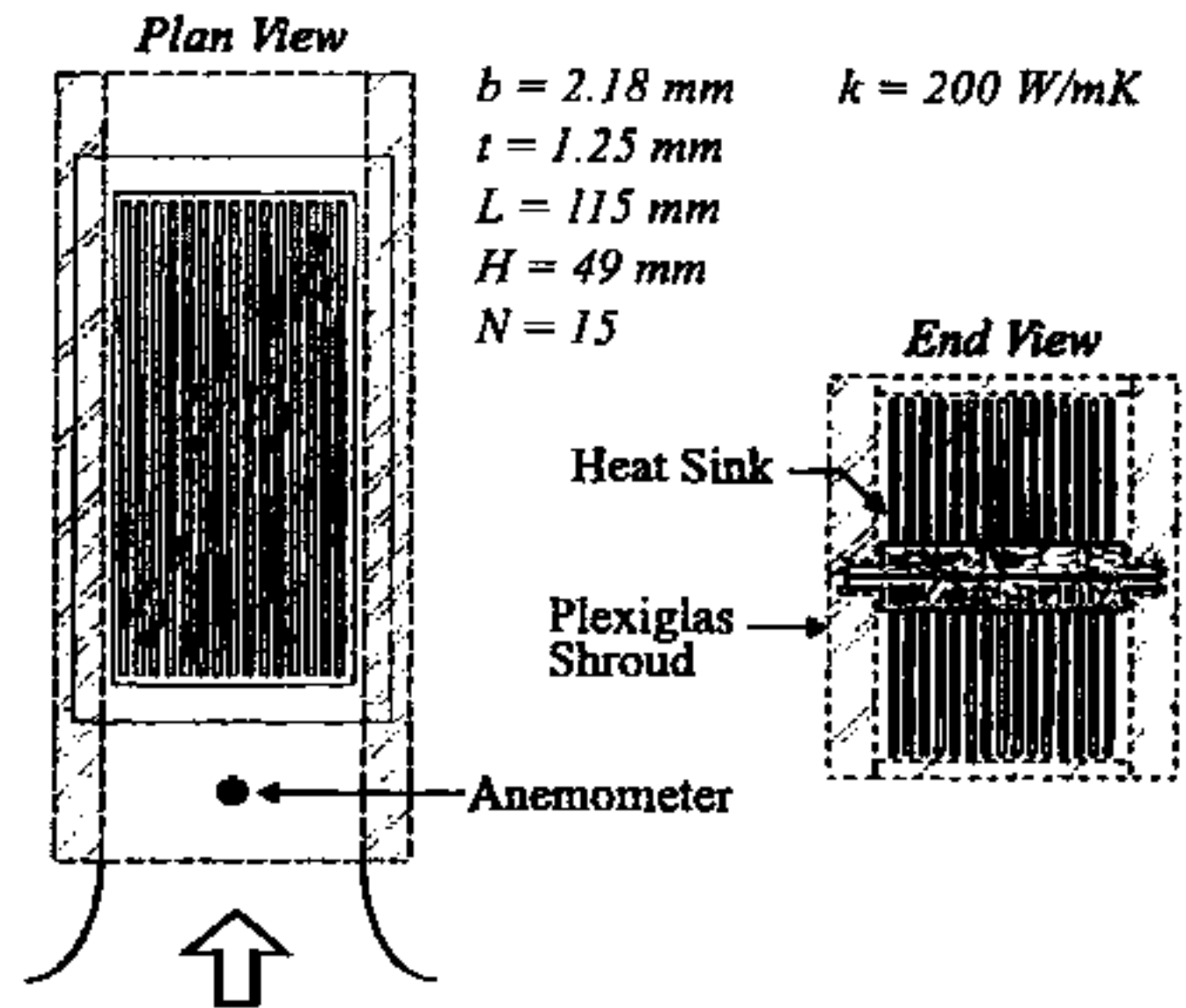


Fig. 6 Schematic of Test Apparatus

where:

$$Nu_i = \left[ \frac{1}{\left( \frac{Re_b^* Pr}{2} \right)^3} + \frac{1}{\left( 0.664 \sqrt{Re_b^*} Pr^{1/3} \sqrt{1 + \frac{3.65}{\sqrt{Re_b^*}}} \right)^3} \right]^{-1/3} \quad (19)$$

## EXPERIMENTAL VALIDATION

Experimental measurements were performed to validate the proposed model using a heat sink prototype with a configuration similar to a commercially-available heat sink for power electronic applications. This high aspect ratio heat sink was tested over a range of velocities and power levels, and the results are compared with model predictions.

### Test Apparatus

To accurately quantify the heat dissipation from the heat sink, matching pairs of heat sinks were configured in a back-to-back arrangement as shown in Fig. 5. The heat sinks were firmly bolted together using six countersunk machine screws located at equal intervals

on the periphery of the assembly. Two 300 W pencil heaters were press fitted into two wells drilled into the baseplates of the heat sinks. Thermal grease, with a thermal conductivity of  $0.8 \text{ W/mK}$  [13], was used between all contacting interfaces of the heat sinks and the pencil heaters. Given the symmetry of the heat sink configuration, it was assumed that all heat dissipated by the pencil heaters was equally distributed between the two heat sinks. The heaters were powered using a 140 VAC variac resulting in typical line voltages of 110 V at a current of approximately 4.5 A. The current flow was sufficiently low that lead losses in the heater wires were minimal.

Temperature measurements were performed using 5 mil T-type copper-constantan thermocouples with a Teflon coating connected to a Fluke Helios datalogger. Because of the small diameter of the thermocouple wires, and the relatively large values of  $Q$ , conductive losses through the leads were assumed to be negligible. Ambient temperatures in the test section were monitored using three thermocouples in various locations. The baseplate temperature was measured using four thermocouples attached to one of the heat sinks at the interface between the baseplates at the locations indicated by  $T_1 - T_4$  in Fig. 6. The thermocouples on the baseplate were located adjacent to and far away from the heaters, such that an arithmetic average of their measured values would provide a representative value for the mean baseplate temperature  $T_b$ . During the testing, the maximum difference in the temperature readings between these four thermocou-

ples was less than 15% of the average value. When the additional spreading effects of the baseplate material are considered, the assumption of a uniform baseplate temperature equal to the average of the measured values is validated.

In order to minimize flow bypass effects, the heat sink assembly was placed inside a Plexiglas shroud, as shown in Fig. 6. The inner dimensions of the shroud were approximately one channel width,  $b$ , larger than the heat sink on all sides, and the baseplate was narrowed at its edges to minimize the contact area between the heat sink and shroud. The shroud and heat sink assembly were suspended at the center of a  $300 \times 300$  mm test section of a vertical, open-ended wind tunnel, and the space between the outside of the shroud and the wind tunnel walls was blocked to control airflow through the assembly. The approach velocity to the heat sink assemblies was measured using a Dantec hot wire anemometer placed approximately 200 mm upstream of the leading edge of the heat sink assembly as shown in Fig. 6.

### Test Procedures and Results

Experimental tests were performed for the following values of approach velocity  $U_a$  and power  $Q_{tot}$ :

$$U_a = 2, 3, 4, 5, 6, 7, 8 \text{ m/s}$$

$$Q_{tot} = 100, 200, 300, 400, 500 \text{ W}$$

where  $Q_{tot} = 100 \text{ W}$  was tested for the lowest value of approach velocity,  $U_a = 2 \text{ m/s}$  only. Each test was allowed to reach a thermal steady state over a three to four hour period, and the results were recorded when the heat sink temperatures remained unchanged for a period of fifteen minutes.

Radiation heat transfer tests were also performed for the heat sink - shroud assembly in a vacuum chamber for a range of power levels. The baseplate and surroundings temperature measurements from these tests were correlated to the form:

$$Q_r = C_1 (T_s^4 - T_a^4) \times 10^{-9} \quad (20)$$

where the value of the coefficient,  $C_1 = 0.537$ , is determined from a fit of the test results. This correlation was used to reduce radiation effects from the results by:

$$Q_{tot} - Q_r$$

In all cases the relative magnitude of the radiation component was less than 1% of the total  $Q_{tot}$ , which is as expected in forced convection.

In order to compare the experimental results with the model predictions, the measured values must be expressed in terms of the dimensionless parameters  $Re_b^*$  and  $Nu_b$ . The channel velocity  $U$  is related to the approach velocity  $U_a$  through a simple, continuity relationship:

$$U = \frac{A_a}{A_o} \cdot U_a \quad (21)$$

where the value for the ratio of the cross sectional areas at the inlet and heat sink sections is  $A_a/A_o = 1.877$ . Once the channel velocity  $U$  has been determined, it can be non-dimensionalized using the previously defined channel Reynolds number, Eq. (7), where the properties are evaluated at the film temperature.

The average Nusselt number for the heat sink is determined by non-dimensionalizing the total heat transfer rate per channel of the heat sink prototype. This per channel heat flow is calculated from the total power dissipation per side (less radiation)  $Q_{tot}/2$ , divided by the number of channels per side,  $N$ , which includes the two half channels formed between the outer fins and the shroud. The Nusselt number is determined by:

$$Nu_b = \frac{\left(\frac{Q/2}{N}\right) b}{k(2LH)(\bar{T}_s - T_a)} \quad (22)$$

where  $\bar{T}_s$  is the mean of the four thermocouple readings on the baseplate.

Figure 7 compares the non-dimensionalized experimental results with the predictions of the proposed model with fin effects included, and the model for the ideal fin,  $\eta = 1$ . The model and the data are in excellent agreement over the full range of  $Re_b^*$ , with an RMS difference of 2.1% and a maximum difference of 6%. The range of channel Reynolds number values shown in Fig. 7 lies between the transition and developing flow regions, and the composite model is very effective in capturing the behavior of the solution for all of the data.

Comparing the two curves shown in Fig. 7 for the model with and without fin effects clearly demonstrates the importance of including the fin efficiency calculation in the analysis, particularly for the long, narrow fins of the test heat sink configuration. Fin efficiency values vary between  $\eta = 0.85$  for the low Reynolds number,  $Re_b^* = 10$ , to  $\eta = 0.75$  for  $Re_b^* = 35$ , where this decrease in  $\eta$  is due to the increase in the convection for larger  $Re_b^*$ .

## REFERENCES

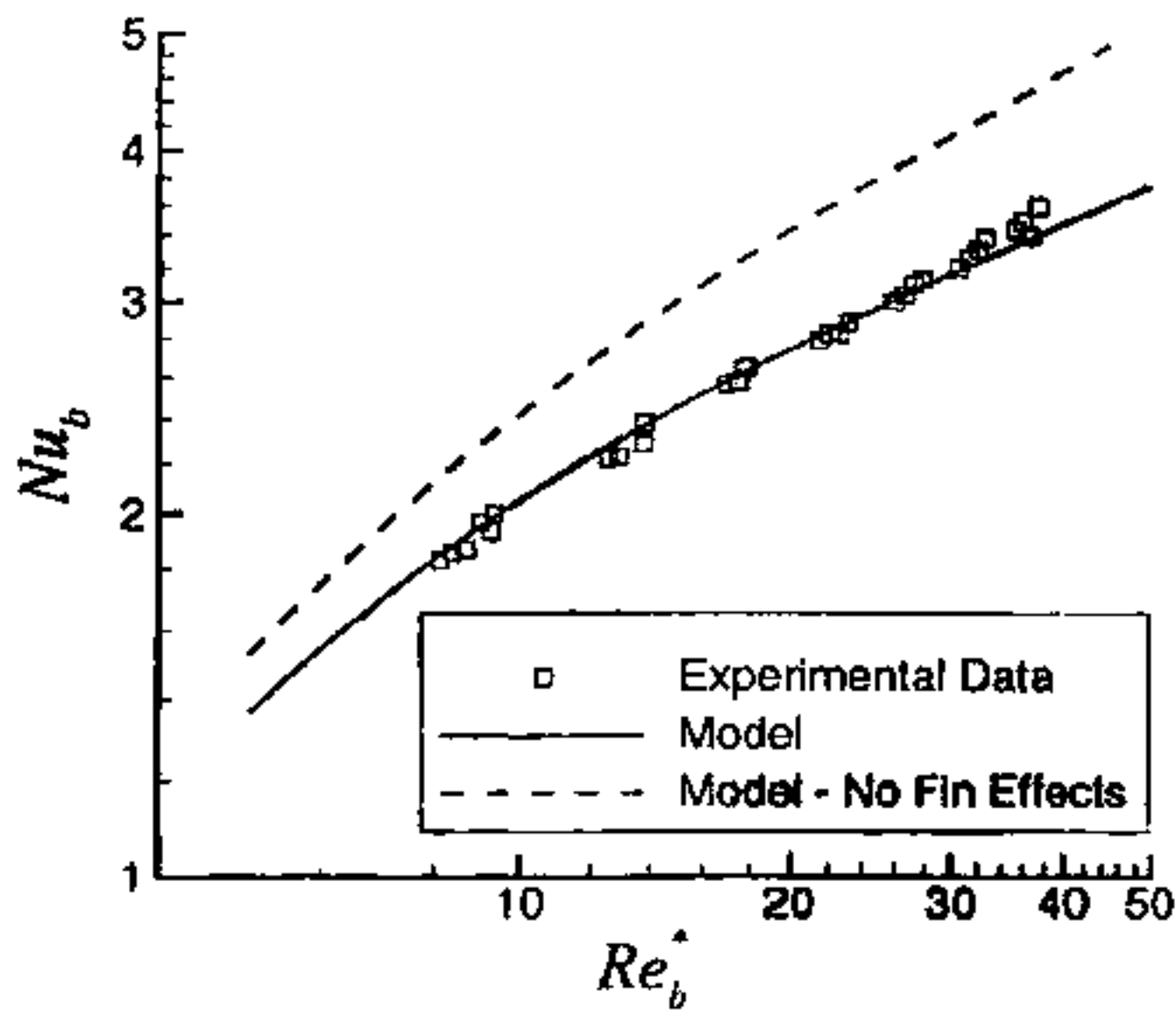


Fig. 7 Comparison of Model with Measured Values

## SUMMARY AND CONCLUSIONS

An analytical model has been developed to predict the average heat transfer rate for forced convection cooled plate fin heat sinks based on a combination of the two limiting cases, fully-developed and developing flow in a parallel plate channel. Fin effects are included in the model to account for temperature variations between the fins and the baseplate, and these fin effects have been shown to be significant in certain heat sink configurations. Measurements were performed for an air cooled, high aspect ratio heat sink prototype, and the model was found to be in excellent agreement with the experimental results, within 2.1% RMS and 6% maximum difference.

The heat sink model presented in this study is limited to configurations where the parallel plate channel assumption is valid, such as in high aspect ratio heat sinks where  $b \ll H$ . Further work is required to include the effects of the baseplate and the shroud for cases where  $b \approx H$ , and to examine flow bypass issues for non-shrouded applications.

## ACKNOWLEDGMENTS

The authors gratefully acknowledge Materials and Manufacturing Ontario and the Natural Sciences and Engineering Research Council of Canada for their continued support of this work.

- [1] Sparrow, E.M., Baliga, B.R. and Patankar, S.V., "Forced Convection Heat Transfer from a Shrouded Fin Array with and without Tip Clearance," *Journal of Heat Transfer*, Vol. 100, No. 4, 1978, pp. 572 - 579.
- [2] Wirtz, R.A., Chen, W. and Zhou, R., "Effect of Flow Bypass on the Performance of Longitudinal Fin Heat Sinks," *Journal of Heat Transfer*, Vol. 116, No. 3, 1994, pp. 206 - 211.
- [3] Shaw, R.K. and London, A.L., *Laminar Flow Forced Convection in Ducts*, Academic Press, New York, 1978.
- [4] Lee, S., "Optimum Design and Selection of Heat Sinks," *IEEE Transactions on Components, Packaging and Manufacturing Technology - Part A*, Vol. 18, No. 4, 1995, pp. 812 - 817.
- [5] Kays, W.M. and London, A.L., *Compact Heat Exchangers*, 3rd. ed., McGraw Hill, New York, 1984.
- [6] Kraus, A.D. and Bar-Cohen, A., *Design and Analysis of Heat Sinks*, John Wiley and Sons, New York, 1995.
- [7] Simons, R.E. and Schmidt, R.R., "A Simple Method to Estimate Heat Sink Air Flow Bypass," *Electronics Cooling*, Vol. 3, No. 2, 1997, pp. 36 - 37.
- [8] Churchill, S.W. and Usagi, R., "A General Expression for the Correlation of Rates of Transfer and Other Phenomenon," *A.I.Ch.E. Journal*, Vol. 18, pp. 1121 - 1128.
- [9] Bejan, A. and Sciubba, E., "The Optimum Spacing of Parallel Plates Cooled by Forced Convection," *International Journal of Heat and Mass Transfer*, Vol. 35, No. 12, 1992, pp. 3259 - 3264.
- [10] Sparrow, E.M., "Analysis of Laminar Forced-Convection Heat Transfer in Entrance Region of Flat Rectangular Ducts," *NACA Technical Note 3331*, 1955.
- [11] Flomerics Inc., 2 Mount Royal Ave., Marlborough, MA, 1999.
- [12] Incropera, F.P. and DeWitt, D.P., *Fundamentals of Heat and Mass Transfer*, 4th. ed., John Wiley and Sons, New York, 1996.
- [13] Aavid Engineering Design Sheet EDS # 116, 1992.